Understanding the physiology of *Lactobacillus plantarum* at zero growth

Philippe Goffin[1,2,3,6], **Bert van de Bunt**[1,2,3], **Marco Giovane**[2,3], **Johan HJ Leveau**[4], **Sachie Höppener-Ogawa**[5], **Bas Teusink**[1,2,3,7,*] and **Jeroen Hugenholtz**[1,2,3,8]

[1] Kluyver Centre for Genomics of Industrial Fermentations, Delft, The Netherlands, [2] Top Institute Food and Nutrition, Wageningen, The Netherlands, [3] NIZO Food Research, Ede, The Netherlands, [4] Department of Plant Pathology, University of California at Davis, Davis, CA, USA and [5] Department of Microbial Ecology, Netherlands Institute of Ecology, Heteren, The Netherlands
[6] Present address: GlaxoSmithKline Biologicals, Rue de l'Institut 89, Rixensart B-1330, Belgium
[7] Present address: Vrije Universiteit Amsterdam (VUA), De Boelelaan 1085, Amsterdam 1081 HV, The Netherlands
[8] Present address: Coca-Cola Europe, Mainburger Strasse 19, Au/Hallerthau 84072, Germany
* Corresponding author. Molecular Cell Biology, IBIVU Systems Bioinformatics, Vrije Universiteit Amsterdam, De Boelelaan 1085, Amsterdam 1081HV, The Netherlands. Tel.: +31 20 598 9435; Fax.: +31 20 598 7229; E-mail: bas.teusink@falw.vu.nl

Situations of extremely low substrate availability, resulting in slow growth, are common in natural environments. To mimic these conditions, *Lactobacillus plantarum* was grown in a carbon-limited retentostat with complete biomass retention. The physiology of extremely slow-growing *L. plantarum*—as studied by genome-scale modeling and transcriptomics—was fundamentally different from that of stationary-phase cells. Stress resistance mechanisms were not massively induced during transition to extremely slow growth. The energy-generating metabolism was remarkably stable and remained largely based on the conversion of glucose to lactate. The combination of metabolic and transcriptomic analyses revealed behaviors involved in interactions with the environment, more particularly with plants: production of plant hormones or precursors thereof, and preparedness for the utilization of plant-derived substrates. Accordingly, the production of compounds interfering with plant root development was demonstrated in slow-growing *L. plantarum*. Thus, conditions of slow growth and limited substrate availability seem to trigger a plant environment-like response, even in the absence of plant-derived material, suggesting that this might constitute an intrinsic behavior in *L. plantarum*.

Molecular Systems Biology **6**: 413 published online 21 September 2010; doi:10.1038/msb.2010.67
Subject Categories: metabolic and regulatory networks; microbiology and pathogens
Keywords: Lactobacillus plantarum; metabolic modeling; retentostat; slow growth; transcriptome analysis

Introduction

In many natural ecosystems, nutrient availability is extremely low, and fluctuates with time. Microorganisms in these environments live a 'feast-and-famine' existence. When conditions are favorable, resources are primarily devoted to growth, whereas under nutrient limitation, most energy is invested in survival (Nyström, 2004). This dichotomy has been formalized by Pirt (1965) in his linear equation for substrate consumption, which states that metabolic energy is divided between the demands of biosynthetic processes (growth) and those of non-growth-associated processes (maintenance). Maintenance energy demand is considered constant for a microorganism under given cultivation conditions. Therefore, when resources are limiting, less energy

becomes available for growth-associated processes, resulting in slow or no growth. These conditions are not only commonly encountered in natural environments, but also in engineered cultivation systems, such as fed-batch fermentations.

Most of the current knowledge about the physiology of slow-growing bacteria is derived from the extensively studied transition from exponential to stationary phase during batch growth, as triggered by nutrient starvation. Metabolism is redirected to alternative substrates and global responses are induced (Redon *et al*, 2005; Hecker *et al*, 2007), among which the stringent response, resulting in the shutdown of growth-associated processes and induction of stress defense mechanisms (Srivatsan and Wang, 2008).

The very fast transition from a rapidly growing to a non-growing state, as observed in batch cultures, is most likely not

very relevant under natural conditions, in which exponential growth at maximum specific growth rate is rarely encountered. In addition, as a result of the high metabolic activity in exponential phase, carbon-starved stationary-phase cells are faced not only with limited nutrient resources, but also with the presence of high concentrations of end products of their own metabolism, which often are growth inhibitory. An alternative model to study bacteria at a defined growth rate is the chemostat, in which the specific growth rate can be directly manipulated by changing the dilution rate, and which provides the additional advantage of a controlled and constant environment. However, chemostats cannot be operated at extremely low dilution rates because of homogeneity problems. This can be overcome by using biomass recycling fermentors (retentostats), that is, chemostats with complete biomass retention. In these systems, biomass progressively accumulates, resulting in decreased specific substrate availability. Hence, less energy is available for growth, and the specific growth rate decreases concomitantly (van Verseveld *et al*, 1984). Such systems have been used to study physiological properties of various microorganisms or microbial communities at low growth rates (Chesbro *et al*, 1979; Arbige and Chesbro, 1982; Müller and Babel, 1996; Konopka *et al*, 1998; Tappe *et al*, 1999). None of these studies, however, has used recently developed genome-scale functional genomics and modeling approaches to study extremely slow-growing bacteria under such conditions.

In this study, *Lactobacillus plantarum* was used as a model microorganism to investigate the physiology of slow growth under retentostat conditions. Besides fermented foods, *L. plantarum* is found in a variety of environmental niches, including plants (Mundt and Hammer, 1968; Ercolani, 1991) and lakes (Yanagida *et al*, 2007), in which nutrient supply is limited (Münster, 1993; Leveau and Lindow, 2001). It has a relatively simple carbon metabolism mainly focused on lactate production, but the genome sequence of strain WCFS1 has revealed a high potential for metabolic flexibility and interactions with the environment (Kleerebezem *et al*, 2003). To get a complete overview of its physiology under these conditions, two genome-scale tools were used: metabolome analysis using a genome-scale metabolic model (Teusink *et al*, 2006) and transcriptome analysis.

Results

Biomass accumulation

L. plantarum WCFS1 was grown under anaerobic retentostat conditions in a chemically defined medium containing glucose and citrate as carbon sources. Two independent cultivations were carried out, which were run for 45 and 31 days (fermentation 1 and 2, respectively). Biomass accumulation followed a negative exponential pattern (Figure 1A), as predicted from the van Verseveld equation (van Verseveld *et al*, 1986). The biomass accumulation profile did not show different modes of growth, as reported for other microorganisms (Chesbro *et al*, 1979; van Verseveld *et al*, 1984; Müller and Babel, 1996). The specific growth rate μ was calculated from the fitted van Verseveld equation (section II.2 of Supplementary information): in the longest-lasting fermentation, the final
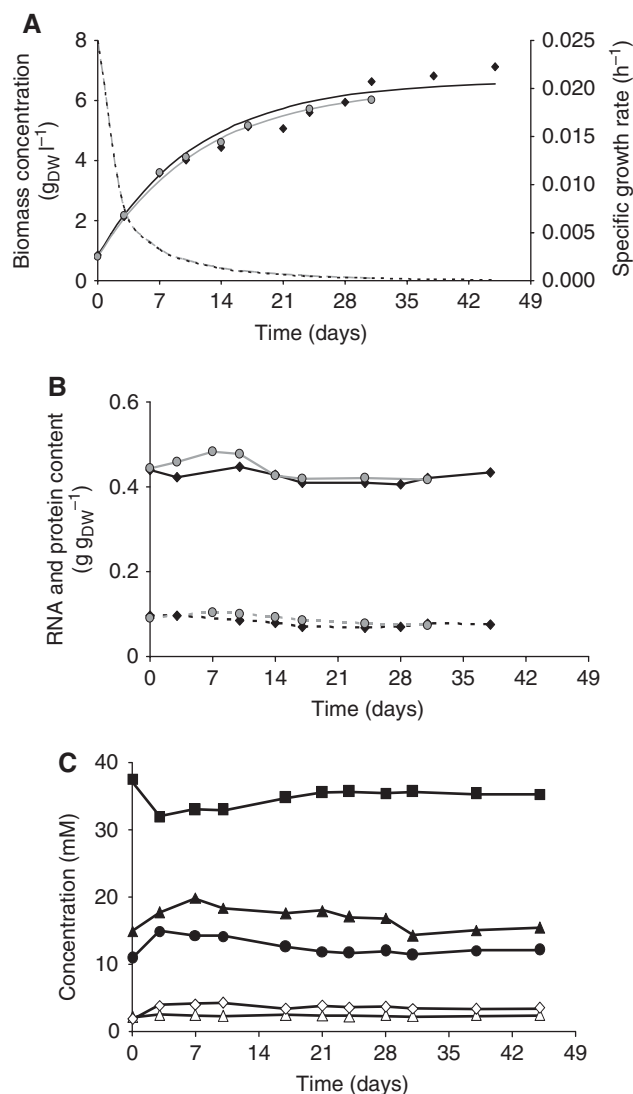
Figure 1 Growth of *L. plantarum* WCFS1 under retentostat conditions. Data from retentostat cultivation 1 and 2 are represented as black diamonds and gray circles, respectively. (**A**) Measured biomass concentration ($g_{DW} l^{-1}$). The biomass calculated from the fitted van Verseveld equation for fermentation 1 (black plain line) and 2 (gray plain line) are shown, as well as the corresponding calculated specific growth rates (black and gray dotted lines for fermentation 1 and 2, respectively). (**B**) RNA (dotted lines) and protein (plain lines) content of the biomass. (**C**) Major end products of metabolism during retentostat cultivation of *L. plantarum* (fermentation 1). Concentrations are expressed as the difference between the measured concentration in the medium feed and the measured concentration in the filter line samples. Closed squares, lactate; closed triangles, acetate; closed circles, formate; open diamonds, ethanol; open triangles, succinate. Source data is available for this figure at www.nature.com/msb.

μ was $0.00006 \, h^{-1}$, corresponding to a calculated doubling time of 1.3 years.

Biomass viability

The van Verseveld equation is based on two assumptions: (i) all biomass is retained inside the fermentor, and (ii) all biomass remains viable and metabolically active (van Verseveld *et al*, 1986). Both conditions were found to be fulfilled under our cultivation conditions. Biomass retention was

higher than 99.99%, as calculated from the ratio of colony-forming units in the fermentor and in the filter line. Viability was assayed using the LIVE/DEAD BacLight kit; the relative fluorescence of the two dyes did not change significantly during retentostat cultivation. Microscopic examination of individual cells revealed no significant changes in cell morphology, such as modification of cell size, increase in cell-chain length, or formation of cell aggregates. No cell debris was observed. Together, these results indicate that retentostat cultivation of *L. plantarum* did not result in a loss of viability. Although metabolic activity was not measured in individual cells, no indication of a decreased metabolism was observed (see below).

Biomass composition

Biomass composition was observed to be constant despite the decreasing growth rate (Figure 1B). RNA and DNA accounted for 7–10 and 2% of the cell mass, respectively, in agreement with previously published values (Teusink *et al*, 2006). The measured protein content accounted for 41–45% of the cell dry weight. The stable RNA and protein content confirmed the metabolically active state of the cells.

Metabolic profile

The two carbon sources present in the medium feed—glucose and citrate—were completely consumed throughout cultivation, confirming that the cultures were carbon and energy limited. Already under chemostat conditions, a mixed acid fermentation pattern was observed. Both fermentations displayed a very similar fermentation pattern, with lactate, acetate, formate, succinate, and ethanol as the main end products (Figure 1C and Supplementary Figure S7a). These compounds accounted for over 99% of the carbon balance at all time points. Minor end products were also detected (Supplementary Figure S1a). Importantly, the overall fermentation pattern did not change significantly during retentostat cultivation (Figure 1C and Supplementary Figure S7a).

Of the 18 amino acids present in the medium feed (no Asn and Gln), only Ser was completely consumed during the whole fermentation. Most amino acids displayed slight variation in their uptake rate. Arg, Asp, Met, and Ala were even produced as the specific growth rate decreased (Supplementary Figure S7c). Ammonia production increased during the first week and then remained stable (Supplementary Figure S7b).

Energy generation under slow-growing conditions

The distribution of energy costs between growth- and maintenance-associated processes was calculated using a genome-scale approach, taking all measured metabolic fluxes into account (Supplementary Figure S2b and section I.3 of Supplementary information; Teusink *et al*, 2006). The calculated values for the maintenance energy coefficient m_{ATP} and the biomass yield Y_{ATP} (0.2351 mmol$_{ATP}$ g$_{DW}^{-1}$ h^{-1} and 0.0160 g$_{DW}$ mmol$_{ATP}^{-1}$, respectively; Supplementary Table S1) indicated that the amount of energy used for maintenance increased from 13 to 94% of the total ATP generated during the

first 31 days of retentostat cultivation ($\mu_{31\ days}$=0.0002 h^{-1}; Supplementary Figure S2c).

The model simulations also provided insight into the mechanisms and limitations of ATP generation. Globally, the predicted pathways of ATP production showed very little variation during retentostat cultivation, as expected from the relatively stable metabolic profile (Figure 1C). The conversion of glucose and citrate to lactate, acetate, ethanol, succinate, and formate was the largest contributor to energy production. Despite a large increase—more than seven-fold—in biomass concentration during retentostat cultivation, the decreased specific substrate availability was not compensated by redirecting the carbon metabolism towards higher ATP-yielding pathways such as increased acetate production.

Role of amino-acid metabolism in energy generation

All the measured fluxes were used as constraints in the genome-scale metabolic model of *L. plantarum*. Using reduced costs as sensitivity parameters on maximal ATP production rate (Teusink *et al*, 2006), the model simulations indicated a negative impact of the uptake of all amino acids—with the exception of Glu—on ATP production during the whole fermentation. Unexpectedly, they did reveal a positive effect of the production of Arg, Asp, Met, and Ala on ATP generation (section I.5 of Supplementary information). As shown in Figure 2A, this effect was connected with the limited ammonium efflux: when no constraint was set on the maximum ammonium production rate, a 15% increase in NH$_4^+$ efflux was predicted, whereas the predicted positive effect (positive scaled reduced cost) of Asp and Met production was drastically reduced, and a strong negative effect of Arg production was predicted. Conversely, the uptake of branched-chain and aromatic amino acids (BCAAs and AAAs, respectively) had a positive effect on ATP production only under conditions of unconstrained ammonium production. Similarly, the production of Ala, as observed from day 31 onward, was predicted to improve ATP production only when ammonium efflux was limiting. These observations indicated that the production of Asp, Arg, Met, and Ala, was connected with the catabolism of BCAA/AAA under conditions of limited ammonium efflux. This was confirmed by performing a simulation in which BCAAs and AAAs were not constrained to be taken up: under such conditions, no positive effect of amino-acid production was predicted (section I.5 of Supplementary information).

Yet, the gain in ATP associated with amino-acid production and the connection with BCAA/AAA consumption were not immediately clear without careful analysis of the modeled flux distributions. Model simulations indicated that BCAAs and AAAs were taken up in significantly higher amounts than needed for biomass (protein) synthesis: at the lowest growth rate investigated ($\mu_{31\ days}$=0.0002 h^{-1}), less than 10% of the total BCAA/AAA uptake flux was sufficient to fulfill biomass requirements, whereas the remaining >90% were predicted to be catabolized. The first step in the catabolism of BCAA/AAA is catalyzed by an aminotransferase, which uses 2-ketoglutarate (2-KG) as the acceptor of the amino group.

This acceptor, 2-KG, can be regenerated through glutamate dehydrogenase (GDH), with concomitant ammonium production (Figure 2B). Thus, an ammonium sink is required to regenerate 2-KG and further catabolize BCAAs and AAAs. This


role can usually be fulfilled by ammonium excretion (Supplementary Figure S3a; Teusink *et al*, 2006). Under retentostat conditions, however, the rate of BCAA/AAA catabolism exceeded the maximum possible flux of 2-KG regeneration through GDH, based on measured ammonium production rates. Therefore, alternative pathways had to be active for supplying the necessary pool of 2-KG without concomitant NH_4^+ generation, to catabolize the excess BCAAs and AAAs.
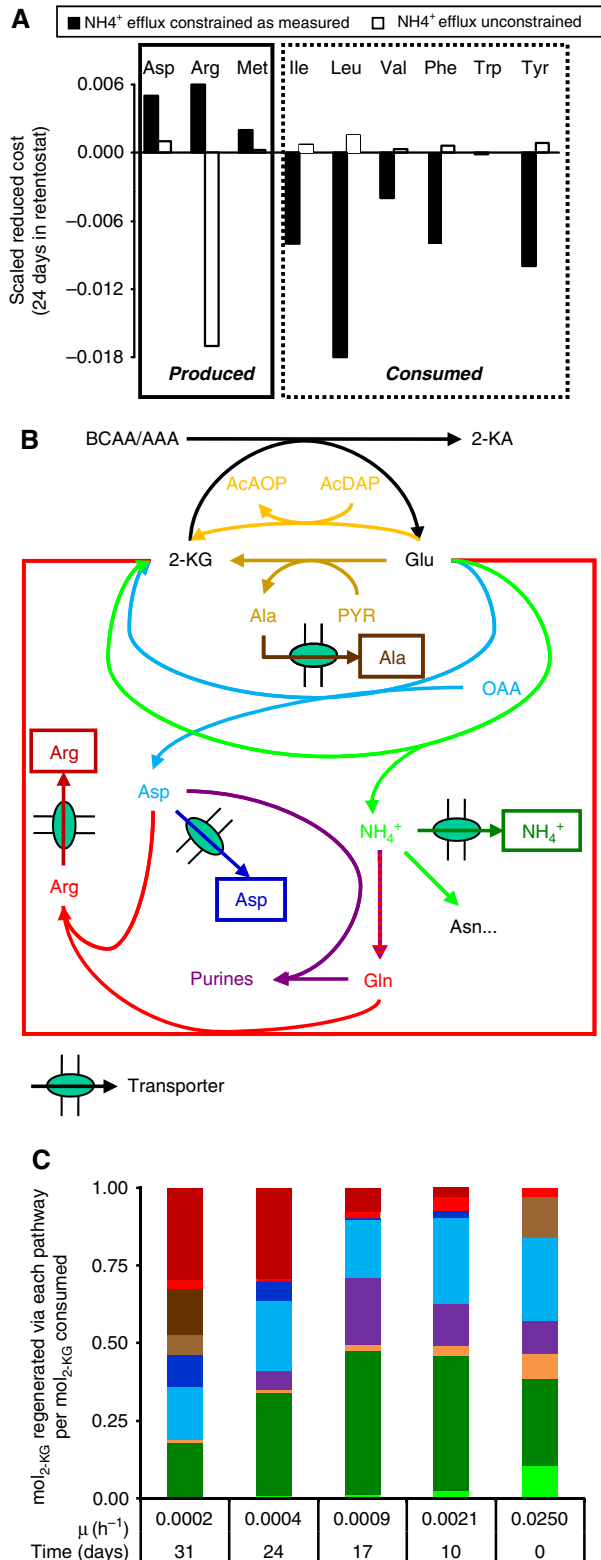
Pathways of 2-ketoglutarate regeneration

To identify the alternative pathways for 2-KG regeneration and to further characterize the role of amino-acid production in the context of BCAA/AAA catabolism and limitation in ammonium efflux, FBA was performed under different sets of constraints (Supplementary Table S2), and the impact of constrained fluxes on the modeled flux distribution was analyzed (section I.5 of Supplementary information and Interactive Slideshow S1). Different solutions were identified that belong to three categories (Figures 2B and 3): (i) higher flux through reactions producing 2-KG by transamination, that is, without production of ammonium, (ii) higher flux through NH_4^+-consuming reactions, allowing a higher flux through GDH, and (iii) lower flux through alternative reactions that consume 2-KG. Production of Asp (reaction [3] in Figure 3) and Ala by transamination from their cognate 2-ketoacid are representative of the first category (Supplementary Figure S3b and e). Met excretion—rather than transamination to 2-keto-4-methylthiobutyric acid (KMBA; reaction [5] in Figure 3)—belongs to the third class. Purine (reactions [1], [9]–[13], and [15] in Figure 3) and Arg biosynthesis (reactions [1] and [7]–[8] in Figure 3) represent a mixed mechanism between the first two categories (Supplementary Figure S3c and d). They

Figure 2 Contribution of amino-acid production to the catabolism of BCAAs and AAAs, and to ATP generation under slow-growing conditions. (**A**) Effect of Arg, Asp, and Met production on ATP generation under conditions of constrained (closed bars) or unconstrained (open bars) ammonium efflux. FBA was used to maximize ATP production, using measured fluxes after 24 days under retentostat conditions (see section I.5 of Supplementary Dataset S1 for details). Scaled reduced costs were calculated as $r_i^* q_i / q_{ATP}$, where q_i represents the flux through reaction i, q_{ATP} is the absolute reduced cost associated with reaction i. Note that Ala production was not included in this graph as it was not observed before 31 days in retentostat conditions. (**B**) Metabolic pathways associated with regeneration of 2-ketoglutarate (2-KG) for the conversion of BCAA and AAA into their cognate 2-ketoacid (2-KA). The color code represents the different solutions used for regenerating 2-KG: green, glutamate dehydrogenase coupled to NH_4^+ efflux (dark green) or to other NH_4^+ dissipation reactions (light green); orange, acetyldiaminopimelate transaminase; light blue, Asp biosynthesis; dark blue, Asp biosynthesis coupled to excretion; purple, purine biosynthesis; light brown, Ala biosynthesis; dark brown; Ala biosynthesis coupled to excretion; red, Arg biosynthesis; dark red, Arg biosynthesis coupled to excretion. Extracellular metabolites are boxed. (**C**) Relative contribution of the different pathways involved in the regeneration of 2-KG produced by the catabolism of BCAA and AAA during the course of retentostat cultivation. The color code is the same as in panel B. The contribution of the different pathways was calculated based on 2-KG regeneration allowed by each pathway, as determined in section I.6 of Supplementary information. The contribution of individual reactions within each pathway is detailed in Supplementary Figure S4. Abbreviations: AcAOP, N-acetyl-L-2-amino-6-oxopimelate; AcDAP, N-acetyl-LL-2,6-diaminopimelate.
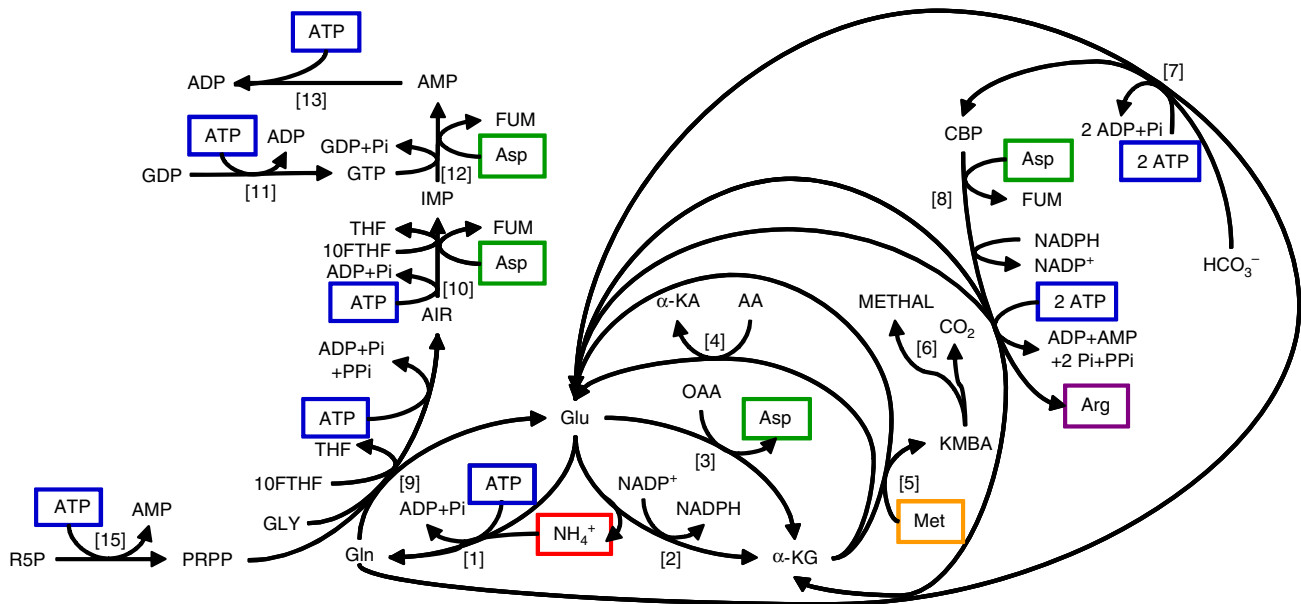
Figure 3 Detailed metabolic map showing the pathways for 2-KG regeneration under retentostat conditions. Numbers between brackets refer to (lumped) reactions (same legend as for Interactive Slideshow S1; see Supplementary Dataset S1 for detailed description of individual reactions): [1], glutamine synthetase; [2], glutamate dehydrogenase; [3], aspartate aminotransferase; [4] branched-chain or aromatic aminotransferase; [5], methionine aminotransferase; [6], 4-methylthio-2-ketobutanoate decarboxylase; [7] carbamoylphosphate synthetase (glutamine-hydrolyzing); [8], lumped reaction of *N*-acetylglutamate 5-phophotransferase (ArgB), *N*-acetylglutamate 5-semialdehyde dehydrogenase (ArgC), *N*-acetylornithine 5-aminotransferase (ArgD), ornithine transacetylase (ArgJ), ornithine carbamoyltransferase (ArgF), argininosuccinate synthase (ArgG), and argininosuccinate lyase (ArgH); [9], lumped reaction of phosphoribosyl-pyrophosphate glutamyl amidotransferase (PurF), phosphoribosyl-glycinamide synthetase (PurD), phosphoribosyl-glycinamide formyltransferase (PurN), phosphoribosyl-formylglycinamide synthetase (PurL), and phosphoribosyl-aminoimidazole synthetase (PurM); [10], lumped reaction of phosphoribosyl-aminoimidazole carboxylase (PurK/PurE), phosphoribosyl-aminoimidazolesuccinocarboxamide synthetase (PurC), adenylosuccinate lyase (PurB), phosphoribosyl-aminoimidazolecarboxamide formyltransferase (PurH), and IMP cyclohydrolase (PurH); [11], nucleoside-diphosphate kinase (Ndk); [12], lumped reaction of adenylosuccinate synthase (PurA) and adenylossucinate lyase (PurB); [13], adenylate kinase (Adk); [15], phosphoribosyl-pyrophosphate synthetase (Prs). Abbreviations: α-KG, 2-ketoglutarate; OAA, oxaloacetate; AA, branched-chain or aromatic amino acid; α-KA, branched-chain or aromatic 2-ketoacid; KMBA, 2-keto-4-methylthiobutyric acid; METHAL, methional; CBP, carbamoylphosphate; FUM, fumarate; PRPP, 5′-phosphoribosyl-1-pyrophosphate; 10FTHF, 10-formyltetrahydrofolate; THF, tetrahydrofolate; AIR, 5′-phosphoribosyl-5-aminoimidazole; R5P, ribose-5-phosphate.

require Gln—produced from Glu and NH_4^+ —as a nitrogen donor (reaction [1]), that is, they act as an ammonium sink (second category), and they also use Asp (reactions [8], [10], and [12])—produced from oxaloacetate by transamination (reaction [3])– as a nitrogen donor, thereby generating additional 2-KG (first category). Arg biosynthesis also involves one aminotransferase reaction, which uses Glu and produces 2-KG (reaction [8]; first category). An additional transamination reaction was also found to have a role in the regeneration of 2-KG (first category): acetyldiaminopimelate transaminase, involved in the biosynthesis of Lys and of the peptidoglycan constituent *m*-diaminopimelate (Figure 2B and section I.6 of Supplementary information). Finally, part of the ammonium produced via GDH was dissipated through alternative reactions such as Asn synthetase (Figure 2B and section I.6 of Supplementary information).

Thus, the production of amino acids by slow-growing *L. plantarum* represented only a fraction of the possibilities provided by its metabolic network, to regenerate 2-KG under conditions in which the flux through GDH was limited, due to limitations in ammonium excretion. Yet, several of these possible alternative pathways were also limited by the dissipation of their end product, in particular when they were involved in the production of biomass precursors. During the course of retentostat cultivation, the alternative solutions

identified through metabolic modeling analysis were sequentially implemented by *L. plantarum* (Figure 2C). Their relative contribution to 2-KG regeneration was calculated from the modeled flux distributions (section I.6 of Supplementary information). At the very beginning of retentostat cultivation, GDH was the main contributor to 2-KG regeneration (40%; Figure 2C), and the NH_4^+ pool was mainly dissipated through excretion. Yet, ammonium excretion was already limiting under these conditions, and alternative pathways such as Asp biosynthesis had to be active for 2-KG regeneration (although Asp excretion was not observed under initial conditions). The contribution of GDH coupled to ammonium excretion slightly increased during the first 10 days—in agreement with the measured increase in NH_4^+ production during this time interval (Supplementary Figure S7b)—before it decreased at lower growth rates (Figure 2C). The contribution of acetyldiaminopimelate transaminase also decreased progressively, in agreement with the decrease in specific growth rate. Indeed, this reaction provides biomass constituents that can only be dissipated through biomass production. Purine biosynthesis increasingly contributed to 2-KG regeneration during the first 17 days, before its contribution declined. Part of the purine synthesized in this way was predicted to be dissipated through the excretion of adenine. At the lowest growth rate investigated, the purine biosynthesis pathway was predicted to carry

no flux (Figure 2C). The regeneration of 2-KG through Asp biosynthesis was relatively constant throughout the course of cultivation (around 25%). However, although all Asp produced was initially re-consumed through biosynthetic pathways (proteins, Asn, or other amino acids; see section I.6 of Supplementary information), an increasing proportion of Asp was excreted as the growth rate decreased. Except under initial conditions, no contribution of Ala biosynthesis was observed before 31 days (Figure 2C), corresponding to the time at which Ala production started to be observed (Supplementary Figure S7c).

Among all pathways used for the regeneration of 2-KG, the most striking evolution during retentostat was observed for Arg biosynthesis. Although it only represented 3% of all 2-KG regeneration at the start of cultivation, it became the major contributor to 2-KG production at the lowest growth rate investigated (33%, including excretion; Figure 2C). Initially, a significant part of the Arg pool was dissipated through protein synthesis, but excretion rapidly became the major Arg dissipation route as the growth rate decreased (Figure 2C), in agreement with the steadily decreasing needs for biomass synthesis.

In the context of energy limitation and high maintenance requirements, the choice of Arg biosynthesis as the major 2-KG regeneration mechanism seems counter-intuitive. Indeed, 6 mol ATP are hydrolyzed for each mol Arg synthesized, resulting in the regeneration of 3 mol 2-KG, that is, 2 mol ATP per mol 2-KG (Figure 3 and equation (7) of Supplementary information). Yet, this solution is energetically more favorable compared to purine biosynthesis (2.5 mol ATP per mol 2-KG; Figure 3 and equation (2) of Supplementary information). Furthermore, considering the situation from the ammonium excretion perspective, the production of 1 mol Arg is equivalent to the excretion of 4 mol NH_4^+, and therefore appears as an efficient alternative under conditions of limited ammonium efflux. Finally, the increasing contribution of less energy-consuming reactions such as Ala biosynthesis at the lowest growth rate (Figure 2C), highlights the metabolic flexibility of *L. plantarum* in this context, and indicates that more energetically efficient solutions are being implemented as the maintenance energy requirement increases.

Global responses during adaptation to slow growth

The gene expression profile was investigated using DNA microarrays at different times during retentostat cultivation, corresponding to increasing amounts of energy used for maintenance purposes, and hence, decreasing specific growth rates.

A high proportion of the genome was found to be differentially regulated at extremely low growth rates (over 25%; Supplementary Table S3). In general, transcriptome analysis failed to reveal the massive induction of global stress responses. First, no stringent response appeared to be triggered, as evident from the absence of downregulation of the majority of genes associated with transcription and genes encoding ribosomal proteins or translation factors (Supplementary Table S4 and Supplementary Dataset S2). This was

confirmed by the constant biomass composition—more particularly, the constant RNA and protein content of the cells (Figure 1B). Second, genes encoding functions involved in other growth-associated processes, such as cell division, DNA replication, or cell wall biosynthesis were usually not repressed (Supplementary Table S4), which correlated with the absence of morphological changes or defects, and the constant biomass viability. Third, a clear general stress response was also not triggered, as deduced from the absence of upregulation of genes encoding alternative sigma factors, and the majority of chaperones and heat, cold, or alkaline shock protein genes (section I.8 of Supplementary information). Altogether, transcriptome profiling correlated with physiological observations indicating that the overall physiology of *L. plantarum* was not fundamentally affected during adaptation to extremely slow-growing conditions, compared to the initial chemostat conditions ($\mu = 0.025\,h^{-1}$). The only stress response observed at low growth rates was the SOS response, with the overexpression of genes involved in DNA replication, recombination, and repair. The most highly induced genes in this category were the genes encoding the Y-family DNA polymerases Pol IV and Pol V (Supplementary Dataset S2).

Correlation between changes in metabolic fluxes and gene expression

The changes in modeled flux distributions, as obtained from FBA (maximization of ATP production), were compared to changes in gene expression (section I.9 of Supplementary information and Supplementary Dataset S3). For the vast majority of reactions, a decrease in flux was observed. This was expected, despite the constant metabolic pattern: because fluxes are specific (per g of biomass), the increase in biomass concentration observed during the course of cultivation resulted in a steadily decreasing specific availability of substrates, and consequently, a lower flux through the pathways using these substrates.

If the flux through these reactions were to be regulated at the gene expression level, a decreased expression of the corresponding genes would have been expected. In total, 88 reactions—32% of the 274 gene-associated reactions carrying a non-zero flux for at least one of the time point considered—were associated with one or more gene(s) that showed a decreased level of expression at low growth rates (Supplementary Dataset S3). Among these, the best correlation was observed for reactions involved in protein synthesis: the expression of half of the tRNA synthetase genes was repressed at low growth rates, in agreement with the well-documented regulation of these genes in response to the availability of the corresponding amino acid (Wels *et al*, 2008). At the level of primary metabolism, several genes encoding enzymes involved in glycolysis, pentose phosphate pathway, tricarboxylic acid cycle, and pyruvate dissipation exhibited a decreased expression level at low growth rates. Intriguingly, although all pyruvate dissipation reactions showed a decreased flux during the course of cultivation, this category contained the highest proportion of upregulated transcripts (Supplementary Table S5). These overexpressed genes corresponded to

reactions associated with more than one gene (acetate kinase, pyruvate formate lyase, and alcohol dehydrogenase), one of the genes being downregulated at low growth rates, whereas another one was upregulated. This suggests the use of alternate isozymes at low growth rates. Similarly, this analysis also suggested the use of alternate pathways (lactate racemase) for the production of D-lactate at low growth rates (section I.9 of Supplementary information).

Similar to what was observed for primary metabolism, the majority of reactions involved in amino-acid metabolism showed a decreased flux as the biomass concentration in the retentostat increased. In this case, a poor correlation was generally observed between changes in flux and changes in gene expression. Furthermore, the production of Arg, Asp, Met, and Ala was mostly not reflected at the transcriptome level. The Arg biosynthesis genes were not upregulated: this was, however, not unexpected as Arg biosynthesis was already active at the start of retentostat cultivation (although no Arg excretion was detected; Figure 2C). As the specific growth rate decreased, Arg started to be excreted (Figure 2C and Supplementary Figure S7c). Accordingly, upregulation of the gene encoding the putative Arg exporter (*lp_1409*) was observed. In a similar vein, the production of Asp and Ala was not correlated with upregulation of the corresponding genes. Similar to the case of Arg, no upregulation of the genes involved in biosynthesis of Asp and Ala was to be expected because they were already produced at the start of fermentation (although not excreted; Figure 2C and Supplementary Figure S7c). Moreover, at the level of export, Asp and Ala are known to be transported through broad-specificity transport proteins (Fernandez and Zuñiga, 2006). Although several genes encoding amino-acid transport proteins were observed to be upregulated at low growth rates (Supplementary Dataset S2), it is extremely difficult to identify which ones are involved in the export of Asp and Ala. Finally, in the case of Met, production of this amino acid resulted from a decreased flux through Met aminotransferase. Correlation was found with decreased expression of genes encoding the branched-chain and aromatic aminotransferases (*bcaT* and *araT1*), which are known to catalyze Met transamination (Fernandez and Zuñiga, 2006). Although upregulation of the Met export system could have been expected, the gene encoding this protein is unknown (section I.9 of Supplementary information).

In conclusion, most metabolic fluxes showed a decrease during retentostat cultivation, due to decreased specific substrate availability resulting from biomass accumulation. This was correlated to decreased gene expression for reactions involved in protein synthesis and primary metabolism. However, relatively poor correlation was observed for amino-acid metabolism.

Interactions with the environment

Another striking feature observed at the level of gene expression was an increased potential for interactions with the environment, potentially with plants. In total, over 50% of genes encoding cell surface proteins displayed significant regulation at low growth rates (15% repressed; 36% induced; Supplementary Table S4), suggesting major modifications of the cell surface. The most highly upregulated genes were observed in the *csc* (cell-surface cluster) gene clusters, six of which being highly induced at low growth rates (over 100-fold; Supplementary Dataset S2). These clusters encode cell-surface protein complexes specifically found in plant-associated gram-positive bacteria, and have been predicted to have a role in the utilization of polysaccharides from plant origin. Expression of these clusters is known to be under control of the carbon catabolite repressor CcpA (Siezen *et al*, 2006). The relief of catabolite repression was also reflected by the regulation of genes involved in the transport and catabolism of alternative carbohydrates. Among these, four gene clusters encoding enzymes for the utilization of β-glucosides—typical sugars from plant origin—were highly upregulated (over 30-fold; Supplementary Dataset S2).

Production of compounds with plant hormone activity

Transcriptome analysis suggested increased interactions with the environment, and particularly with plants. An *in silico*-based metabolic approach was used to study the potential of slow-growing *L. plantarum* for producing compounds involved in plant interactions. This approach was based on the fact that FBA requires all balances to be closed. Therefore, non-measured end products can be suggested.

Most possible end products as predicted with this approach were derived from the catabolism of BCAAs and AAAs (section I.7 of Supplementary information). Many of the reactions involved in BCAA and AAA catabolism are common, and the corresponding enzymes are known to have broad substrate specificity (Fernandez and Zuñiga, 2006). A number of these compounds were indeed produced, confirming that these catabolic pathways were active under conditions of slow growth. In particular, phenylacetaldehyde and indole compounds were detected (Supplementary Figures S5 and S6a). Model simulations also predicted the conversion of Met to methional, with KMBA as an intermediate. The observed production of methanethiol (Supplementary Figure S5), which can be generated non-enzymatically from KMBA or methional (Smit *et al*, 2005; Fernandez and Zuñiga, 2006), indicated that this pathway was active in slow-growing *L. plantarum*.

Interestingly, a number of indole compounds derived from Trp, as well as phenylacetate derived from Phe or phenylacetaldehyde, are known to elicit auxin-like responses in plants (Woodward and Bartel, 2005). The compound, KMBA, has been previously identified as the precursor of the plant stress hormone ethylene in several microorganisms (Ince and Knowles, 1986). Thus, metabolic analysis pointed to a possible production of plant hormones—or precursors thereof—in slow-growing *L. plantarum*. To verify this hypothesis, supernatants from retentostat cultivation were assayed for their effect on radish root development. As shown in Figure 4, a significant reduction in length was observed when roots were treated with samples collected from retentostat after 10 days ($\mu=0.0021\,h^{-1}$), corresponding to the highest measured concentration of indole compounds (Supplementary Figure S6a). The inhibition of radish root development by retentostat samples demonstrates that slow-growing *L. plantarum* produces compounds that interact with the plant physiology,
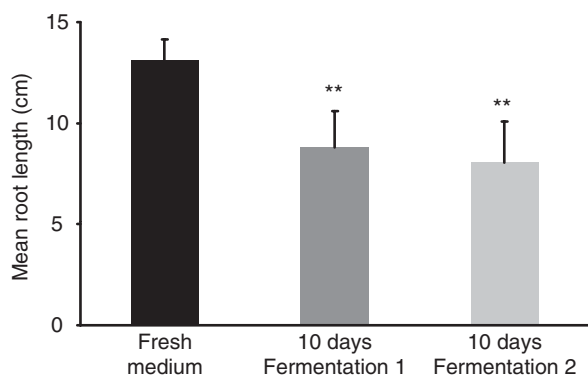
Figure 4 Inhibition of radish root development by supernatants of *L. plantarum* after 10 days under retentostat conditions. Radish root assays were performed according to Leveau and Lindow (2005). Samples were diluted 10,000 times. Error bars represent the s.d. values. **Highly significantly different from fresh medium ($P < 0.01$ Tukey test).

as deduced from the *in silico* metabolic modeling approach, and in line with results from transcriptome analysis showing the upregulation of genes involved in the catabolism of plant-derived material.

Discussion

The adaptation of *L. plantarum* to extremely slow growth under limited carbon and energy supply was studied at two different levels: the transcriptome and metabolome. Detailed measurements of metabolic fluxes were performed, and were used as constraints in a genome-scale metabolic model, to precisely calculate the amount of substrate and energy used for net biomass synthesis and for maintenance. This approach also provided insights into the mechanisms and limitations of ATP production. In parallel, transcriptome analysis was used to investigate the global cell response to such conditions.

Slow growth as studied here is fundamentally different from the widely studied carbon starvation-induced stationary phase. Indeed, non-growing cells in retentostat conditions are glucose-limited rather than starved, and the transition from a growing to a non-growing state under retentostat conditions is progressive, in contrast with the abrupt transition in batch cultures. These differences were reflected in various aspects of the cell physiology. Unexpectedly, our data indicate that the physiology of virtually non-growing *L. plantarum* under glucose-limited retentostat is very similar to that of faster growing cells in continuous culture, even under conditions in which maintenance accounts for over 90% of all energy expenses.

The metabolic behavior was remarkably stable during adaptation to slow growth. Similar to what is observed upon glucose starvation, transcriptome analysis revealed the upregulation of genes for the utilization of alternative carbohydrates (lactose, cellobiose, sucrose, and β-glucosides) at low growth rates in *L. plantarum*. This observation reflected the relief of catabolite repression, and indicated that extremely slow-growing cells were prepared for glucose starvation. However, as glucose was still present and no alternative

carbohydrates were fed to the cells, the energy metabolism remained glucose based. Glucose was mainly converted to lactate, even in slow-growing cells. Previous studies of retentostat cultivation of lactic acid bacteria at higher growth rates also reported a relatively stable metabolic profile with lactate as the major end product (Major and Bull, 1989; Hjörleifsdottir *et al*, 1991; Yoo *et al*, 1997). In this study, we show that this unexpectedly stable and energetically inefficient metabolic behavior can be extended to virtually non-growing *L. plantarum*. The constant metabolism over a wide range of specific growth rates indicates that extreme carbon limitation and slow growth are not the trigger for a metabolic shift towards higher ATP-yielding pathways, as also reported for *Lactococcus lactis* (Koebmann *et al*, 2002). Yet, even if lactic acid production seems energetically inefficient in the absence of oxygen, this behavior might be beneficial in natural environments such as plant leaves, in which oxygen is present and would allow *L. plantarum* to further convert lactate into acetate through the pyruvate oxidase-dependent pathway (Goffin *et al*, 2006), yielding additional energy.

Physiological processes related to maintenance comprise energy costs associated with defense mechanisms or turnover of macromolecules (Tempest and Neijssel, 1984). Under our conditions, defense mechanisms were not massively induced. In particular, analysis of biomass composition and gene expression failed to reveal clear stringent or general stress responses, which are generally observed in glucose-starved cells, in which they correlate with a global shutdown of functions associated with growth (Koburger *et al*, 2005; Redon *et al*, 2005). Owing to the dramatic decrease in specific growth rate during retentostat cultivation of *L. plantarum* (over 100-fold), a downregulation of genes involved in growth-associated functions would have been expected at extremely low growth rates. However, this was generally not observed, in particular for RNA and protein synthesis. Several key genes involved in transcription were even upregulated (Supplementary Table S4). These observations suggest that active transcription and translation are required to account for the observed stable biomass composition.

Slow-growing *L. plantarum* also exhibited an apparent increased potential for genetic diversity, as indicated by the upregulation of the two error-prone DNA polymerases and the absence of downregulation of the transcriptional machinery. The induction of mechanisms such as error-prone replication or transcription-mediated mutations, results in increased rates of mutagenesis under non-growing conditions (Robleto *et al*, 2007). Diversity was however not apparent in retentostat-grown *L. plantarum*: no significant heterogeneity of colony size or morphology was observed at extremely low growth rates. Changes in cell morphology such as observed during long-term starvation (cell aggregates, filamentous cells; Finkel (2006)), were not detected, and samples isolated from slow-growing *L. plantarum* under retentostat conditions did not display modified growth behavior when cultivated under batch conditions (data not shown). Interestingly, preliminary data indicate that perturbations such as complete glucose starvation during slow-growth in the retentostat result in the selection of mutants with modified growth capabilities (P. Goffin, unpublished data). We conclude from this that the selection pressure that favors mutants able to use alternative

energy sources must be significantly lower in the retentostat than during stationary phase, probably because cells are glucose limited, but not starved.

Another important response of *L. plantarum* to extremely slow growth was an increased potential for interactions with the environment, particularly with plants, which was revealed by the combination of metabolic modeling and transcriptome analyses. *A priori*, the production of the amino acids Arg, Asp, Met, and Ala, seemed energetically inefficient. Previous studies in *L. plantarum* (Teusink *et al*, 2006) or *L. lactis* (Oliveira *et al*, 2005) reported the failure of FBA to predict inefficient (overflow) metabolism such as lactic acid production. In this study, provided the appropriate fluxes were constrained, FBA was found to accurately explain how the production of amino acids positively contributed to ATP generation. At a fixed ammonium efflux—fixed at the measured value—reduced cost analysis showed that BCAAs and AAAs are expensive to metabolize, and that coupling the catabolism of BCAAs and AAAs to the production of the abovementioned amino acids has a positive effect on the energetics of the cell. This is an excellent example in which precise, quantitative modeling results in new insights in physiology that intuition would never have achieved.

This observation raises two important questions. First, why would NH_4^+ efflux be limited? It is possible that the availability of ammonium transporters in the cell membrane might limit its export. The observed overexpression of a high number of cell surface and membrane protein genes at low growth rates could result in membrane crowding. It could thus be beneficial to excrete ammonium in the form of amino acids, which can be translocated by broad-specificity transporters that are present for other purposes. An alternative hypothesis could be connected to the well-documented toxicity of ammonium ions in bacteria (Buurman *et al*, 1991), yeast (Hess *et al*, 2006), and plants (Cao *et al*, 1993; Szczerba *et al*, 2008) at low potassium concentrations. Ammonium is probably not toxic for *L. plantarum* under the conditions studied here, as the K^+ concentration is high (180 mM) and *L. plantarum* has been shown to grow in the presence of very high NH_4^+ concentration (Nicaise *et al*, 2008). However, *L. plantarum* could be intrinsically 'programmed' not to produce high amounts of NH_4^+ under conditions of slow growth, such as those encountered in its natural habitat, in which it is found in association with plants (Mundt and Hammer, 1968; Ercolani, 1991). Production of amino acids could represent an alternative to NH_4^+ excretion, as also observed in yeast, in which biosynthesis and excretion of amino acids has been identified as a detoxification mechanism against high NH_4^+ concentrations (Hess *et al*, 2006).

The second question raised by the observation of amino-acid production is: why are BCAAs and AAAs catabolized in excess if they do not generate energy? A possible answer lies in the end products of their catabolism, a number of which could serve as signaling molecules for the interaction of *L. plantarum* with its environment. Model simulations predicted the production of precursors of plant hormones, and supernatants from retentostat-grown *L. plantarum* inhibited plant root development. The metabolic analysis thus suggests that these compounds are not simple by-products of amino-acid catabolism, providing a possible explanation for the presence of flavor-forming pathways in *L. plantarum*: the production of plant hormones—or hormone precursors—under conditions of slow growth might be a way to divert the plant metabolism towards its own interest. Indeed, the production of auxin compounds is a common strategy used by plant pathogens to increase local substrate availability on plant leaves (Beattie and Lindow, 1999). In support of this view, four gene clusters involved in the utilization of β-glucosides—typical sugars from plant cell-wall degradation—and six of the nine *csc* clusters—predicted to have a role in the utilization of plant polysaccharides (Siezen *et al*, 2006)—were highly induced at extremely low growth rates.

Traditionally, there are two main types of culture systems to study bacterial evolution during long-term cultivation (Finkel, 2006). On one hand, systems such as chemostats or serial batch cultures maintain a (relatively) constant environment. They can be used for the selection of mutants with altered growth capabilities, such as improved growth on poor substrates, and several studies have reported the predictive power of metabolic modeling in this context (Fong and Palsson, 2004; Herring *et al*, 2006; Teusink *et al*, 2009). However, such systems result in a constant loss of genetic diversity. On the other hand, in long-term stationary phase cultures, genetic diversity is maintained, but the environment evolves constantly, resulting in the constant selection of mutants able to use alternative sources of carbon and energy (Finkel, 2006). Although such conditions are probably more relevant from an environmental point of view, the constantly changing conditions severely limit the applicability of metabolic modeling approaches to predict adaptation behaviors. Thus, as pointed out by Finkel (2006), using the current long-term cultivation models, there is a tradeoff between maintaining a constant environment with genetic bottlenecking (chemostats or serial batch cultures) versus maintaining genetic diversity in an ever-changing environment (long-term stationary phase). Alternating conditions of low substrate availability and starvation are likely to be common in natural environments, and the retentostat offers an alternative that combines the advantages of all other systems, allowing the study of long-term genetic variation under tightly controlled, environmentally relevant conditions.

In conclusion, the physiology of *L. plantarum* at extremely low growth rates, as studied by genome-scale metabolic modeling and transcriptomics, is fundamentally different from that of starvation-induced stationary phase cells. Excitingly, these conditions seem to trigger responses that favor interactions with the environment, more specifically with plants. The reported observations were made in the absence of any plant-derived material, suggesting that this response might constitute a hardwired behavior.

Materials and methods

Strain and culture conditions

L. plantarum WCFS1 was cultivated at 30°C in a chemically defined medium (Teusink *et al*, 2006) containing 25 mM glucose. A 2.0-l fermentor (Applikon Biotechnology, The Netherlands) with 1.5 l working volume was inoculated with an exponentially growing preculture. The fermentor was operated under anaerobic conditions (nitrogen atmosphere) at a stirring speed of 200 r.p.m., and pH was

regulated at 5.5 with NaOH 5 M. At an $OD_{600\,nm}$ of 0.7, the feed pump was switched on and the fermentor was operated in chemostat mode (dilution rate $D=0.025\,h^{-1}$) until steady-state was achieved (six volume changes, as judged by constant $OD_{600\,nm}$). The culture was then switched to retentostat conditions, while keeping the dilution rate constant, that is the spent medium was eliminated through a 0.22-μm polypropylene filter (AppliSense sample filter assembly, Applikon Biotechnology, The Netherlands) fully immersed in the culture medium. To ensure a constant working volume in the fermentor, a conductivity contact positioned at the surface of the liquid triggered a peristaltic pump, which removed the filtrate at a rate equivalent to the dilution rate.

Metabolic profile

Sampling, metabolite determination, and analysis of biomass composition were performed as described in section II.1 of Supplementary information. The parameters of the van Verseveld equation (van Verseveld *et al*, 1986) were fitted to the measured dry weight, and the specific growth rate was calculated from the fitted equation. Metabolic fluxes were calculated from the measured metabolite concentration and the calculated dry weight (section II.2 of Supplementary information).

Metabolic model and constraint-based modeling

The metabolic model used in this study was derived from Teusink *et al* (2006), with slight modifications as described in section II.3 of Supplementary information. The exact version of the model used in this study is provided as Supplementary information (Model S1). A different biomass equation was used for every time point in each retentostat, to adapt the stoichiometric coefficients for RNA, protein, and DNA, to the measured values (section II.3 of Supplementary information). The coefficients of all other biomass components were assumed to be identical to previously calculated values (Teusink *et al*, 2006).

Flux balance analysis and flux variability analysis (FVA) were carried out using the Simpheny™ software (Genomatica, San Diego, CA). Measured metabolic fluxes for amino acids (Ala, Arg, Asn, Asp, Cys, Gln, Glu, Gly, His, Ile, Leu, Met, Phe, Pro, Ser, Thr, Trp, Tyr, and Val), sugars (glucose, fructose, lactose, maltose, mannose, mannitol, sorbitol, and sucrose), organic compounds (acetate, citrate, L-lactate, D-lactate, pyruvate, formate, acetoin, ethanol, succinate, acetaldehyde, malate, and 2,3-butanediol), and ammonia were used as constraints in the model (lower and upper bounds set at -10% and $+10\%$ of the measured flux, respectively), unless otherwise indicated. For Lys, the minimal uptake flux was set at 0.0. This was necessary because the only sink for Lys in the model—Lys tRNA synthetase—was not sufficient to account for the measured Lys uptake flux at extremely low growth rates. However, using this constraint, no Lys uptake was predicted; rather, all Lys required for biomass (protein) synthesis was produced through the Lys biosynthetic pathway (because it allows regeneration of 2-KG). To reflect at least partially the fact that Lys uptake was observed, an additional constraint was introduced in the model, so that the Lys uptake flux had to be equal to the flux through Lys tRNA synthetase. No oxygen exchange was allowed, to reflect the anaerobic conditions. For compounds that were present in the fresh medium but not measured, the lower bound was defined as the maximum possible uptake flux (complete consumption), and the upper bound was set at $+\infty$. For non-measured compounds that were not present in fresh medium, the lower bound was set at 0 and the upper bound was set at $+\infty$.

Determination of the energy-related maintenance coefficient (m_{ATP}) and biomass yield (Y_{ATP})

The energy parameters m_{ATP} and Y_{ATP} were calculated using the genome-scale model, as previously described (Teusink *et al*, 2006). This approach is based on the assumption that all energy produced under steady-state energy-limited conditions, is used for anabolic processes (full coupling). In the modified Pirt equation used for the genome-scale modeling approach ($q_{ATP}=m_{ATP}+\mu[x+y]$, with $[x+y]=Y_{ATP}^{-1}$), ATP costs are explicitly distributed between energy requirements for the biosynthesis of precursors (x), assembly of these precursors into new cells (y), and maintenance (m_{ATP}) (Teusink *et al*, 2006). To calculate x and y separately, FBA was performed in which y was set as 0 in the biomass equation, and instead an ATP-dissipating reaction was introduced in the model (Teusink *et al*, 2006). The maximum flux through this reaction was calculated at every time point from each retentostat cultivation. The maximal ATP production calculated by the model simulations under these conditions represented $q_{ATP,y}$, the amount of ATP required for the assembly of biomass components into new cells. In the linear relationship between $q_{ATP,y}$ and μ, the slope represented y, and the intercept with the y-axis represented m_{ATP}. The calculated values of y and m_{ATP}, as well as the reduced cost associated with biomass synthesis, representing x, were introduced in the modified Pirt equation, to calculate the total amount of ATP generated by the cells (q_{ATP}) at each time point. Values of q_{ATP} were plotted against μ to calculate Y_{ATP} (slope^{-1}) and m_{ATP} (intercept with the y-axis; Supplementary Figure S2b, closed circles and plain line). As the two retentostat cultivations resulted in essentially similar metabolic patterns (section I.10 of Supplementary information), data from both fermentations were treated together for the calculation of Y_{ATP} and m_{ATP}.

Study of the impact of ammonium efflux, amino-acid production, and amino-acid catabolism, on ATP generation

Flux balance analysis was performed to maximize the flux through the abovementioned ATP dissipating reaction, using measured fluxes from fermentation 1 after 24 days as constraints (model and constraints provided as Supplementary information (Model S1)). The different simulations were performed under different sets of constraints for ammonia, Asp, Arg, Met, and/or BCAA/AAA exchange fluxes, as detailed in Supplementary Table S2 and section I.5 of Supplementary information.

Prediction of non-measured metabolic end products

Flux variability analysis was performed on the flux distributions determined by FBA (maximization of ATP production) to explore the space of possible solutions (i.e. the range of flux values (span) for each reaction in the model) compatible with the experimental constraints. This was performed for every time point from each retentostat cultivation. For exchange reactions, the maximum possible concentration of the corresponding metabolite at every time point was calculated from the maximal flux values, as follows: $[i]_{(t),max}=(x_t q_{i(t),max})/D$, where $[i]_{(t),max}$ is the maximal predicted concentration of metabolite i at time t (mM), x_t is the biomass concentration at time t ($g_{DW}\,l^{-1}$; calculated from the fitted van Verseveled equation), $q_{i(t),max}$ is the maximal flux for exchange of metabolite i at time t (mmol $g_{DW}^{-1}\,h^{-1}$; calculated by FVA), and D is the dilution rate (0.025 h^{-1}).

Transcriptome analysis

The protocol used for microarray analysis is described in section II.4 of Supplementary information. Hybridization was performed on custom designed *L. plantarum* WCFS1 11K Agilent oligo microarrays (GEO accession number GPL5874). Significantly regulated probes were defined based on a *P*-value <0.05 and a fold change higher than 2.0. Genes for which all significantly regulated probes did not show the same trend and genes for which more than 50% of the probes were not significantly regulated, were considered not regulated. For the remaining genes, the fold change was calculated as the average of the fold change between significantly regulated probes. The normalized transcriptome data have been deposited in the GEO database (accession no. GSE18340).

Supplementary information

Supplementary information is available at the *Molecular Systems Biology* website (http://www.nature.com/msb).

Acknowledgements

Conflict of interest

The authors declare that they have no conflict of interest.

References

Arbige M, Chesbro W (1982) Very slow growth of *Bacillus polymyxa*: stringent response and maintenance energy. *Arch Microbiol* **132:** 338–344

Beattie G, Lindow S (1999) Bacterial colonization of leaves: a spectrum of strategies. *Phytopathology* **89:** 353–359

Buurman E, Teixeira de Mattos M, Neijssel O (1991) Futile cycling of ammonium ions via the high affinity potassium uptake system (Kdp) of *Escherichia coli*. *Arch Microbiol* **155:** 391–395

Cao Y, Glass A, Crawford N (1993) Ammonium inhibition of *Arabidopsis* root growth can be reversed by potassium and by auxin resistance mutations *aux1*, *axr1*, and *axr2*. *Plant Physiol* **102:** 983–989

Chesbro W, Evans T, Eifert R (1979) Very slow growth of *Escherichia coli*. *J Bacteriol* **139:** 625–638

Ercolani G (1991) Distribution of epiphytic bacteria on olive leaves and the influence of leaf age and sampling time. *Microb Ecol* **21:** 35–48

Fernandez M, Zuñiga M (2006) Amino acid catabolic pathways of lactic acid bacteria. *Crit Rev Microbiol* **32:** 155–183

Finkel SE (2006) Long-term survival during stationary phase: evolution and the GASP phenotype. *Nat Rev Microbiol* **4:** 113–120

Fong SS, Palsson BO (2004) Metabolic gene-deletion strains of *Escherichia coli* evolve to computationally predicted growth phenotypes. *Nat Genet* **36:** 1056–1058

Goffin P, Muscariello L, Lorquet F, Stukkens A, Prozzi D, Sacco M, Kleerebezem M, Hols P (2006) Involvement of pyruvate oxidase activity and acetate production in the survival of *Lactobacillus plantarum* during the stationary phase of aerobic growth. *Appl Environ Microbiol* **72:** 7933–7940

Hecker M, Pane-Farre J, Volker U (2007) SigB-dependent general stress response in *Bacillus subtilis* and related gram-positive bacteria. *Annu Rev Microbiol* **61:** 215–236

Herring CD, Raghunathan A, Honisch C, Patel T, Applebee MK, Joyce AR, Albert TJ, Blattner FR, van den Boom D, Cantor CR, Palsson BO (2006) Comparative genome sequencing of *Escherichia coli* allows observation of bacterial evolution on a laboratory timescale. *Nat Genet* **38:** 1406–1412

Hess D, Lu W, Rabinowitz J, Botstein D (2006) Ammonium toxicity and potassium limitation in yeast. *PLoS Biol* **4:** e351

Hjörleifsdottir S, Holst O, Mattiasson B (1991) Effects on product formation in *Lactococcus lactis* 65.1 in continuous culture with complete cell recycling. *Bioprocess Eng* **6:** 29–34

Ince S, Knowles C (1986) Ethylene formation by cell-free extracts of *Escherichia coli*. *Arch Microbiol* **146:** 151–158

Kleerebezem M, Boekhorst J, van Kranenburg R, Molenaar D, Kuipers O, Leer R, Tarchini R, Peters S, Sandbrink H, Fiers M, Stiekema W, Lankhorst R, Bron P, Hoffer S, Groot M, Kerkhoven R, de Vries M, Ursing B, de Vos W, Siezen R (2003) Complete genome sequence of *Lactobacillus plantarum* WCFS1. *Proc Natl Acad Sci USA* **100:** 1990–1995

Koburger T, Weibezahn J, Bernhardt J, Homuth G, Hecker M (2005) Genome-wide mRNA profiling in glucose starved *Bacillus subtilis* cells. *Mol Genet Genomics* **274:** 1–12

Koebmann B, Solem C, Pedersen M, Nilsson D, Jensen P (2002) Expression of genes encoding F_1-ATPase results in uncoupling of glycolysis from biomass production in *Lactococcus lactis*. *Appl Environ Microbiol* **68:** 4274–4282

Konopka A, Zakharova T, Oliver L, Paseuth E, Turco R (1998) Physiological state of a microbial community in a biomass recycle reactor. *J Ind Microbiol Biotechnol* **20:** 232–237

Leveau J, Lindow S (2001) Appetite of an epiphyte: quantitative monitoring of bacterial sugar consumption in the phyllosphere. *Proc Natl Acad Sci USA* **98:** 3446–3453

Leveau J, Lindow S (2005) Utilization of the plant hormone indole-3-acetic acid for growth by *Pseudomonas putida* strain 1290. *Appl Environ Microbiol* **71:** 2365–2371

Major N, Bull A (1989) The physiology of lactate production by *Lactobacillus delbrueckii* in a chemostat with cell recycle. *Biotechnol Bioeng* **34:** 592–599

Müller R, Babel W (1996) Measurement of growth at very low rates ($\mu >=0$), an approach to study the energy requirement for the survival of *Alcaligenes eutrophus* JMP 134. *Appl Environ Microbiol* **62:** 147–151

Mundt J, Hammer J (1968) Lactobacilli on plants. *Appl Microbiol* **16:** 1326–1330

Münster U (1993) Concentrations and fluxes of organic carbon substrates in the aquatic environment. *Antonie van Leeuwenhoek* **63:** 243–274

Nicaise C, Prozzi D, Viaene E, Moreno C, Gustot T, Quertinmont E, Demetter P, Suain V, Goffin P, Deviere J, Hols P (2008) Control of acute, chronic, and constitutive hyperammonemia by wild-type and genetically engineered *Lactobacillus plantarum* in rodents. *Hepatology* **48:** 1184–1192

Nyström T (2004) Growth versus maintenance: a trade-off dictated by RNA polymerase availability and sigma factor competition? *Mol Microbiol* **54:** 855–862

Oliveira AP, Nielsen J, Forster J (2005) Modeling *Lactococcus lactis* using a genome-scale flux model. *BMC Microbiol* **5:** 39–53

Pirt S (1965) The maintenance energy of bacteria in growing cultures. *Proc R Soc Lond B Biol Sci* **163:** 224–231

Redon E, Loubiere P, Cocaign-Bousquet M (2005) Transcriptome analysis of the progressive adaptation of *Lactococcus lactis* to carbon starvation. *J Bacteriol* **187:** 3589–3592

Robleto E, Yasbin R, Ross C, Pedraza-Reyes M (2007) Stationary phase mutagenesis in *B. subtilis*: a paradigm to study genetic diversity programs in cells under stress. *Crit Rev Biochem Mol Biol* **42:** 327–339

Siezen R, Boekhorst J, Muscariello L, Molenaar D, Renckens B, Kleerebezem M (2006) *Lactobacillus plantarum* gene clusters encoding putative cell-surface protein complexes for carbo-hydrate utilization are conserved in specific gram-positive bacteria. *BMC Genomics* **7:** 126–138

Smit G, Smit B, Engels W (2005) Flavour formation by lactic acid bacteria and biochemical flavour profiling of cheese products. *FEMS Microbiol Rev* **29:** 591–610

Srivatsan A, Wang J (2008) Control of bacterial transcription, translation and replication by (p)ppGpp. *Curr Opin Microbiol* **11:** 100–105

Szczerba M, Britto D, Ali S, Balkos K, Kronzucker H (2008) NH_4^+-stimulated and -inhibited components of K^+ transport in rice (*Oryza sativa* L.). *J Exp Bot* **59:** 3415–3423

Tappe W, Laverman A, Bohland M, Braster M, Rittershaus S, Groeneweg J, van Verseveld H (1999) Maintenance energy demand and starvation recovery dynamics of *Nitrosomonas europaea* and *Nitrobacter winogradskyi* cultivated in a retentostat with complete biomass retention. *Appl Environ Microbiol* **65:** 2471–2477

Tempest DW, Neijssel OM (1984) The status of Y_{ATP} and maintenance energy as biologically interpretable phenomena. *Annu Rev Microbiol* **38:** 459–486

Teusink B, Wiersma A, Molenaar D, Francke C, de Vos W, Siezen R, Smid E (2006) Analysis of growth of *Lactobacillus plantarum* WCFS1 on a complex medium using a genome-scale metabolic model. *J Biol Chem* **281:** 40041–40048

Teusink B, Wiersma A, Jacobs L, Notebaart RA, Smid EJ (2009) Understanding the adaptive growth strategy of *Lactobacillus plantarum* by *in silico* optimisation. *PLoS Comput Biol* **5:** e1000410

van Verseveld H, Chesbro W, Braster M, Stouthamer A (1984) Eubacteria have 3 growth modes keyed to nutrient flow. Consequences for the concept of maintenance and maximal growth yield. *Arch Microbiol* **137:** 176–184

van Verseveld H, De Hollander J, Frankema J, Braster M, Leeuwerik F, Stouthamer A (1986) Modeling of microbial substrate conversion, growth and product formation in a recycling fermentor. *Antonie van Leeuwenhoek* **52:** 325–342

Wels M, Groot KT, Kleerebezem M, Siezen RJ, Francke C (2008) An *in silico* analysis of T-box regulated genes and T-box evolution in prokaryotes, with emphasis on prediction of substrate specificity of transporters. *BMC Genomics* **9:** 330–345

Woodward A, Bartel B (2005) Auxin: regulation, action, and interaction. *Ann Botany* **95:** 707–735

Yanagida F, Chen Y-S, Yasaki M (2007) Isolation and characterization of lactic acid bacteria from lakes. *J Basic Microbiol* **47:** 184–190

Yoo I-K, Chang H, Lee E, Chang Y, Moon S-H (1997) By-product formation in cell-recycled continuous culture of *Lactobacillus casei*. *Biotechnol Lett* **19:** 237–240